SYNTHESIS AND FIELD EMISSION RESPONSE OF ANODICALLY REDUCED GRAPHENE OXIDE

A DISSERTATION

Submitted in partial fulfilment of the

requirements for the award of the degree

of

MASTER OF TECHNOLOGY

in

METALLURGICAL AND MATERIALS ENGINEERING

(With specialization in Physical Metallurgy)

by

NIKHIL MOHANDAS

DEPARTMENT OF METALLURGICAL AND MATERIALS ENGINEERING

INDIAN INSTITUTE OF TECHNOLOGY ROORKEE

ROORKEE – 247667 (INDIA)

MAY 2016

CANDIDATES DECLARATION

I hereby declare that the work presented in the dissertation entitled **"Synthesis and field emission response of anodically reduced graphene oxide"** submitted in partial fulfilment of the requirements for award of the degree of **Master of Technology** in **Metallurgical and Materials Engineering, Indian Institute of Technology Roorkee,** is an authentic record of my work carried out under the supervision of **Dr. Indranil Lahiri,** Assistant Professor, Department of Metallurgical and Materials Engineering, Indian Institute of Technology Roorkee. The matter embodied in this has not been submitted by me in any other degree.

Nikhil Mohandas

Enrolment No. 14545009

Department of Metallurgical and Materials Engineering

Date:

CERTIFICATE

This is to certify that the above statement made by the candidate is correct to the best of my knowledge.

Dr. Indranil Lahiri

Supervisor

Assistant Professor

Department of Metallurgical and Materials Engineering

Indian Institute of Technology Roorkee

ACKNOWLEDGEMENT

I take this opportunity with much pleasure to thank all the people who have helped me through the course of my journey towards producing this dissertation.

It is my proud privilege to express my foremost acknowledgement and sincere thanks to my supervisor **Dr. Indranil Lahiri** for his splendid guidance during my M Tech project. I thank him for believing in my ability and supporting me equally well during both downfalls and successes of my project work. I have certainly grown both as a person and a professional under his guidance and will cherish forever the excellent learning experience that I had during the last year.

I would also like to thank **Dr. Debrupa Lahiri** for providing me with the essential facilities required for the completion of my work.

I sincerely acknowledge **Dr. S. K. Nath** former Head and **Dr. Anjan Sil**, Head, Metallurgical and Materials Engineering, Indian Institute of Technology Roorkee, for providing me with all the facilities needed for the completion of my M Tech work.

Acknowledgements are also due to my mentors **Mr Vijayesh**, **Mr Rajkumar** and my labmates **Ms Gurjinder** and **Ms Kavitha** for their precious advice and consistent support during my work.

I am deeply thankful to my M Tech co-workers **Mr Sathish** and **Mr Mukul** for their constant support during my good and bad times.

I would like to thank my classmates **Mr Ajay**, **Mr Surinder**, **Mr Neeraj**, **Mr Vipin**, **Mr Vignesh Mr Diwan** and **Mr Rakesh**. I had a wonderful time with all of you.

I am pleased to thank **Mr R. S. Sharma**, lab assistant, metallography lab and **Mr R. K. Sharma** to give me necessary support and information required for my work.

Finally, this dissertation would not have been possible without the confidence, inspiration and support of my family. Their unconditional love and care is my only driving force towards my goals. At last but not the least I am thankful to the almighty for continuously guiding me in inexplicable ways and providing me with the courage and drive for all of my endavours.

Nikhil Mohandas

ABSTRACT

Reduced graphene oxide (RGO) has in recent studies proven to be a suitable contender for electron field emission owing to high field enhancement due to high aspect ratio and atomically thin edges. Graphene thin films for field emission have been prepared by using numerous solution-based deposition techniques such as membrane filtration, dip coating, spray-coating, spin coating etc. Among these methods, Electrophoretic deposition (EPD) stands advantageous due to factors such as easy setup and scalability, high adhesion, thickness control and high uniformity. In most of these studies the graphene is reduced before deposition, reduction is mainly controlled chemically by hydrazine hydrate or thermally. In-situ film deposition and simultaneous anodic reduction of graphene oxide (GO) platelets using EPD has already been reported. Our study focuses on deposition of GO on various metallic substrates and investigation of the extent of reduction of GO (prepared using improved hummers method) under varying EPD parameters such as time, voltage of deposition, electrode gap, electrode material and their respective field emission behaviour. Attempts were also made to improve the field emission response of the RGO films by further controlled reduction of these films. Field emission current as high as 2.7 mA/cm^2 and lowest turn field of 1.5 V/μm were achieved.

Keywords: reduced graphene oxide, thin films, field emission.

TABLE OF CONTENTS

TITLE **PAGE NO.**

LIST OF FIGURES

LIST OF TABLES

1. Introduction

Carbonaceous nanomaterials such as carbon nanotubes, graphene and fullerenes have successfully found a profound status in research during the past few decades. With minute tailoring of structure and morphology they have been applied to a wide range of devices including field emission, conducting polymer, composite material, thermal interface material, super capacitors, electrodes for Li ion batteries etc. [1-6]. Graphene made its appearance in about a decade ago. Unique properties such as high conductivity, mechanical strength, flexibility and transmittance have attracted extensive interest in this field [7]. Due to its vital applications, extensive research has been carried out on the scalable synthesis of graphene with defect free structure at feasible costs. These methods include mechanical exfoliation [8], chemical vapour deposition (growth) [9], chemical exfoliation etc. among the above methods chemical exfoliation stands most economical as it uses graphite as the precursor material. It involves oxidation of graphite flakes using improved hummers method followed by ultra sonication to obtain graphene oxide. It is further reduced using suitable method to obtain reduced graphene oxide [10].

Owing to removal of functional groups during reduction of graphene oxide, large number of defects are introduced in the RGO sheet surfaces. These defects result in deterioration of properties of graphene. oxygen functional groups present on the basal plane of GO renders it electrically insulating and has to be reduced in order to use it for electronic applications [11].Common methods used for reduction of GO are thermal, chemical, electrochemical etc [12,14]. reduction with chemical agents such as hydrazine hydrate are time consuming and have very low yield whereas, thermal reduction results in higher concentration of structural defects due to rapid reduction [13]. In the present work we use anodically reduced graphene oxide for enhanced field emission applications. Electrophoretic deposition of GO results in in-situ reduction at the anode [15].

1.1. Motivation

Presence of large amount of oxygen functional groups on the basal planes of graphene oxide making it electrically insulating due to large work function. In order to reduce its work function reduction has to be carried out [16]. Research has been done on versatile reduction methods including chemical reduction, thermal reduction, laser assisted reduction, electrochemical reduction etc. [17]. The primary focus of research is to find a cost effective method which is efficient and can be readily scaled up. An *et. al*. reported thin film fabrication and simultaneous anodic reduction of graphene oxide using electrophoretic deposition (EPD) method [15]. EPD offers economical route for deposition of charged entities dispersed in liquid media. Advantages of this method include low cost setup, uniform deposition easy scalability [18].

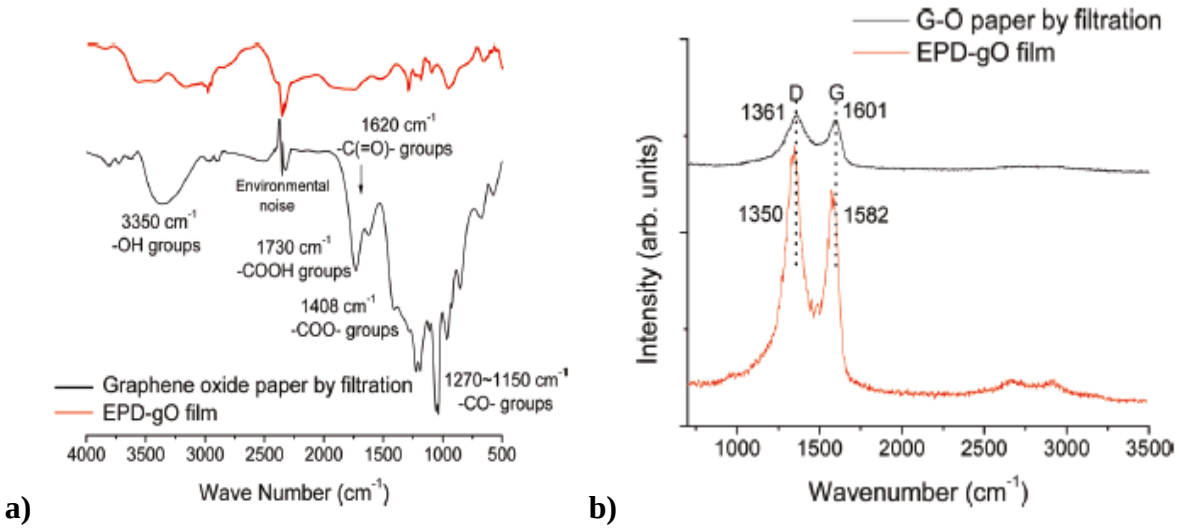

Fig. 1: a) FT-IR and b) Raman plots of GO paper and EPD-GO film confirming the reduction of GO during EPD [15].

The report states that deprotonated carboxylic groups assign negative charge to the GO platelets. These platelets are attracted towards anode and when contact happens, the functional group is oxidised resulting in release of CO_2 and formation of covalent bond between de-functionalised carbon atoms. The Raman as well as FT-IR spectra of as prepared GO paper and EPD reduced graphene oxide provides requisite proof for the reduction of graphene oxide. Conventionally, RGO thin film preparation involves multiple steps, such as reduction, washing (to remove contaminants) and subsequent deposition usually done using EPD[19]. The EPD reduction offers single step preparation of graphene thin films. The RGO film obtained by the above method can be utilised for various conductive thin film applications such as solar cells, super capacitors etc.

1.2. Objective

The primary objective of the present research is to study and optimize the field emission response of RGO produced using EPD on conducting substrates. Simultaneously it is important to study the dependence of the extent of reduction and field emission response on the various EPD parameters such as voltage, electrode gap and solution concentration. During the study a number of attempts were made to enhance the emission current from the prepared graphene films including further reduction of RGO films using thermal reduction and hydrazine hydrate vapour reduction.

2. Literature Review

2.1. Graphene

Graphene represents two dimensional sp^2 bonded carbon structure. It is resembles carbon nanostructures possessing six member carbon rings such as carbon nanotubes (CNT), and fullerenes but has distinct structural difference owing to stability of two dimensional sheet structure. Pristine graphene exhibits exceptionally high electron mobility of over 2000 cm^2/V s, a yield strength of 0.5-1 T Pa and an intrinsic strength of 300-400 N/m [20]. Unique properties such as quantum Hall effect at room temperature and ballistic conduction of charge carriers has triggered immense research interest in graphene in the last decade. According to number of layers graphene can be divided into single-layer graphene, bilayer graphene and few-layer graphene (<10 layers) [21].

2.2. Graphene Oxide and Reduced Graphene Oxide

In spite of the convincing properties of pristine graphene, owing to extensively high cost of synthesis, it is difficult to utilize it for any application. For research purpose, a structurally poorer form of graphene called graphene oxide is used. It is obtained by chemical oxidation of natural graphite using strong oxidizing agents [10]. Oxidation results in the introduction of oxygen functional groups such as carboxyl, hydroxyl, carbonyl and epoxy on the basal planes of graphite increasing the inter layer spacing from 3.3 nm to ~7 nm. This reduces the inter layer Van Der Waal attraction and favours the exfoliation of graphene sheets by ultra sonication. Presence of oxygen functional groups on the surface of graphene oxide renders it electrically insulating [22]. The insulating nature of graphene oxide can be accounted by the formation of carbon oxygen dipoles on various C-O bonds present in different chemical surroundings resulting in high work function. The conductivity of graphene oxide can be regained by reduction of graphene oxide resulting in the removal of oxygen functional groups from basal planes, thus reducing the work function [21]. The various methods used for the reduction of graphene oxide are discussed in the next section. Only partial recovery of electronic and mechanical properties is possible during reduction of graphene oxide. This is due to the introduction of high density of structural defects during reduction [23].

2.3. Reduction of graphene oxide

2.3.1. Thermal Reduction

Thermal reduction simply involves heating of graphene oxide to temperatures ranging from 200^{o}C to 1100^{o}C under vacuum, inert or reducing atmosphere. In the initial stages of research rapid heating rates up to 2000^{o}C/ min were used to accomplish both exfoliation and reduction to obtain graphene from graphene oxide. As the graphene oxide is heated, the oxygen functional groups break down to give gases such as CO and CO_2 [17]. The residual carbon radicals so formed recombine to regain the parent graphitic structure. During rapid heating the so produced gases exert immense pressure (>2.5 MPa) on the graphite oxide layers resulting in the exfoliation of stacked layers [23]. A recent work by Zhao *et. al.* reported the increase in the C/O ratio of graphene oxide during inert annealing of graphene oxide. The C/O ratio increased from 3.77 to 8.55 from 200^{o}C to 900^{o}C [24]. Even though thermal annealing appears to be fast and efficient method for reduction of graphene oxide but comes with a number of disadvantages. The release of carbonaceous gases during reduction consumes carbon atoms from the surface of graphene oxide rendering the graphene basal plane rich in defects.

2.3.2. Chemical Reduction

Chemical reduction of graphene oxide involves chemical reaction of graphene oxide with strong reducing agents such as hydrazine monohydrate, sodium borohydride or hydriodic acid. Reduction is carried out at near room temperature treatment of graphene oxide in liquid media generally deionized water. Reduction of graphite oxide with hydrazine was discovered well before the discovery of graphene and has proved to be the most efficient reducing agent. For hydrazine reduction 1ml of hydrazine hydrate is to be added to 100ml of 1mg/ml GO aqueous solution. The system has to be maintained at 100^{o}C under ice bath for about 24h. Graphene oxide loses its hydrophilic nature due to removal of surface functional groups and agglomerates followed as black mass at the bottom of the container. This has to be followed by multiple steps of washing to remove the residual reducing reagent. C/O ratio can be consistently increased up to 10.3 using this method [25]. Along with efficient reduction hydrazine offers reduced graphene oxide with lower defect density. This can be explained using the reduction mechanism. During reduction firstly the various functional groups are first reduced and subsequently removed upon further reduction.

H.A. Becerill *et .al.* reported the reduction of graphene oxide powder using hydrazine monohydrate vapour. They reported the optimal reduction conditions to be 40oC and 22 hrs. reduction [26]. The reduction turned the powder from black to metallic grey. Effective reduction of graphene oxide has been reported using sodium borohydride and hydriodic acid. Some unconventional methods for reduction of graphene oxide such as microwave reduction, photo reduction, and laser assisted reduction have also been reported [17].

2.4. Field electron emission

2.4.1. Field emission theory

Field electron emission refers to cold cathode electron emission from atomically thin emission sites fabricated on cathode under the application of ultrahigh electrostatic field carried out in a highly evacuated atmosphere. Fig. 2 shows the basic setup for field electron emission. The atomically thin edges on the emitters result in enhancement of electric field due to local field enhancement owing to bending of electron bands resulting in electrons tunnelling through potential barrier. Nano scale materials such as nanotubes, nanoribbons, nanobelts and nanorods of both inorganic materials such as molybdenum oxide, tungsten oxide, copper oxide, and organic materials such as graphene and carbon nanotubes [40] prove to be suitable candidates for field emission.

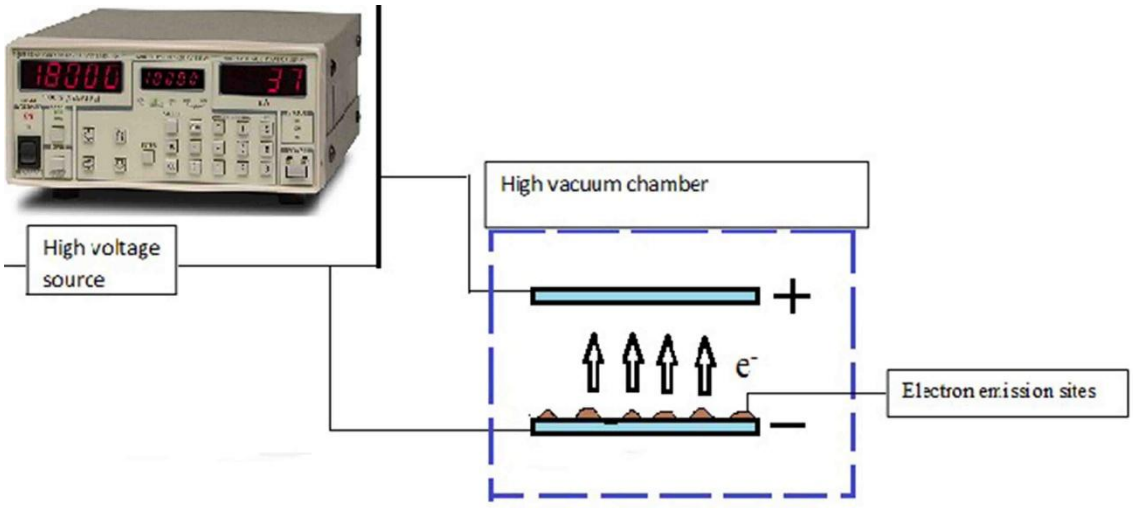

Fig. 2: Basic setup for electron field emission.

Field emission can be explained by Fowler Nordheim tunnelling and electron energy band diagram. Unlike thermionic emission [42] in field emission electrons do not require any external energy excitation. Electrons are filled up to Fermi energy level. The energy difference

between Fermi level and an electron in vacuum is called work function (φ). Generally order to eject an electron it has to be provided with an energy equal to φ. When an external field is applied between electrons, the potential energy of electron reduces outside the metal as shown in Fig. 3.

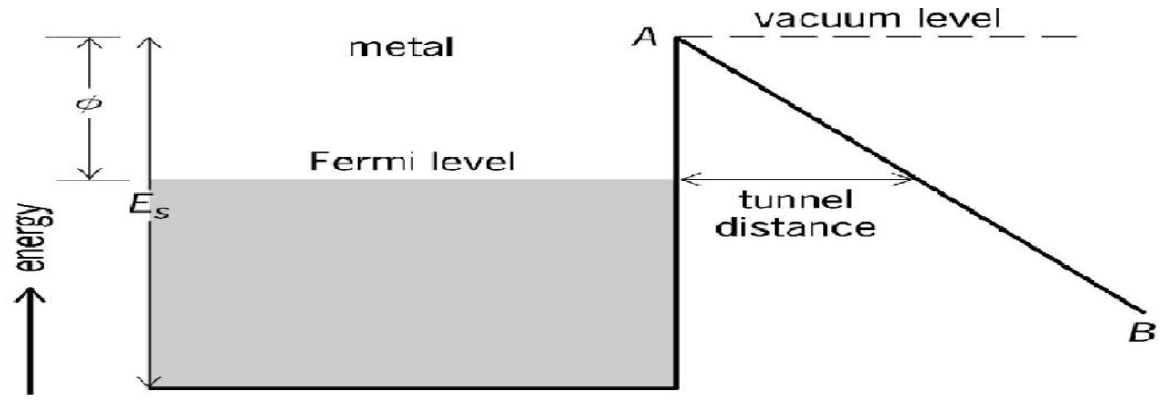

Fig. 3: Fowler-Nordheim tunnelling band diagram [42].

When sufficient external field is applied the potential energy of vacuum becomes equal to the Fermi energy level of the metal and electrons can tunnel through this barrier without any excitation. As the external field increases the vacuum potential drops continuously resulting in exponential increase in tunnelling current.

The main factors that apply to field electron emission are morphology of emission sites (aspect ratio), work function of emitter, density distribution of emission sites, area of effective electron emission and extent of vacuum generated. Field enhancement refers to the generation of higher effective field than externally applied field due to accumulation of charge at atomically thin edges of emission sites.

2.4.2. Field emission characteristics

Field enhancement factor (**B**) can be calculated by using the following expression [42]:

$$\mathbf{Ln(1/E^2) = \frac{Ln(A\alpha\beta^2/\varphi) - B\varphi^{3/2}}{\beta E}} \quad \rightarrow \textbf{(EQ-1)}$$

A & B =constants

α = effective emission area

β = field enhancement factor

φ = work function of emitter

E = applied field

The emission current density (**J**) can be given by the following expression [42]:

$$\mathbf{J = AE^2 exp\left\{-\frac{\beta}{E}\right\}} \quad \rightarrow \textbf{(EQ-2)}$$

The field emission behaviour of any material is studied with the help of the following two plots:

Current density vs. electric field plot:

This plot exhibits the variation of emission current with increase in the externally applied field. Generally an emission current density of 10 μA/cm^2 is considered as the turn on current and the corresponding field is called turn on field. A good field emitter should a low turn on field and high maximum current density.

Fowler Nordheim plot (F-N plot):

The F-N plot mostly forms a linear curve. F-N plot stands as high importance as it provides a convenient method to calculate the field enhancement factor. The slope of Ln (1/E^2) vs 1/E curve (k) has an inverse ratio to the field enhancement factor β [43]:

$$k = -\frac{B\varphi^{3/2}}{\beta}, \quad \rightarrow \textbf{EQ. 3}$$

Current stability plot:

This plot exhibits the field emission performance of an emitter over long periods of use. Consistent emission current must be exhibited by the emitter for it to be suitable for various applications. Current stability test can vary from few seconds to hours.

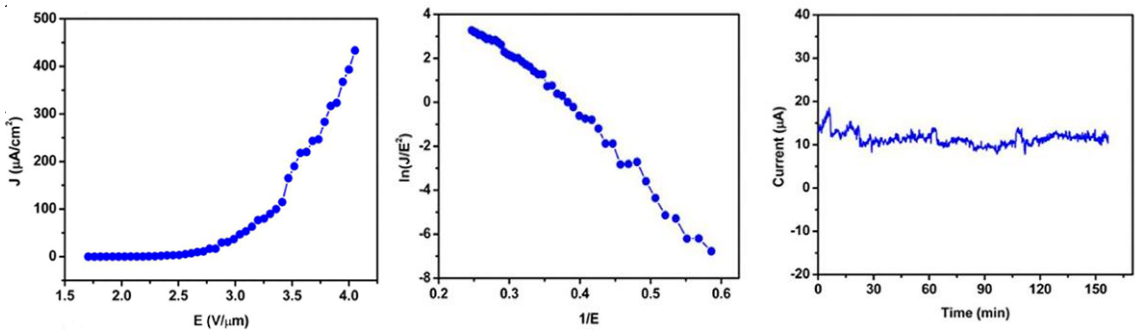

Fig. 4: Typical current density, Fowler–Nordheim and current stability plot [37].

2.5. Reduced graphene oxide as field emitters

Owing to its atomically thin edges, high electrical conductivity, thermal stability and high aspect ratios graphene structures have proved a well-established candidate for field emission research in the last decade. Wide scale research has been done in order to understand the field emission response of reduced graphene oxide and study its dependence on its chemical functionalization, orientation and structure. Despite of structural defects and existent work function excellent emission currents as high as 200mA/cm^2 and turn on field as low as 0.1 v/μm have already been reported [27-28]. The key to better emission properties relies mainly on the following factors. Firstly, controlling the defect density on basal planes of RGO introduced during synthesis. Secondly, controlling the number of layers in the as synthesized RGO. Thirdly, providing the optimum orientation in order to attain good field enhancement. Fourthly, regulating the carbon to oxygen ratio in RGO to obtain suitably low work function. Huang *et. al.* reported the variation of turn on field for RGO with the change in C/O ratio. In the same work the simultaneous reduction of RGO during field emission owing to joule heating effect was reported [1].

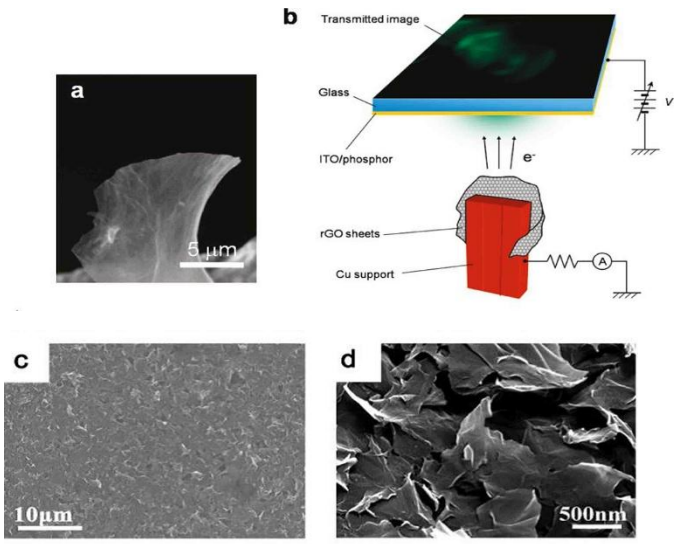

Fig. 5: a) and b), FE-SEM image and setup to test field emission behaviour from edge of monolayer RGO [28]. c) and d)RGO film prepared on ITO glass for field emission [33].

Field emission for RGO on different substrates including metallic, semiconductor and conductive tapes. Conductive substrates prove more efficient for field emission as it ensures availability of sufficient electrons for field emitters attached to it. Field emission characteristics have been tested for RGO deposited on copper (sheet, grid and tape), ITO glass and carbon conducting tape. Conducting tape substrates poses added advantages of flexible samples and good emitter substrate adhesion. Good emitter adhesion proves important for field emission as it permits the application of higher local fields with reduced chance of emitter detachment and possibility of a short circuit. Using semiconducting material as substrates for field emitters results in escalated turn on fields and lower emission currents attributable to the unavailability of sufficient electrons in the conduction band [29]. This issue can be overcome by using highly n doped semiconductor or by providing metal transition layer between the semiconductor and emitters [03, 31]. Despite of the disadvantages mentioned above, semiconductors provide the flattest substrates and better adhesion for testing field emission characteristics and cannot be neglected. Due to their sheet structure and atomically thin edges it becomes important to study the dependence of field emission behaviour on the orientation of field emission. RGO deposited on any substrate preferably adheres parallel to the substrate resulting in low field enhancement factor. A number of methods have been used to overcome this including orientational polymer composites and RGO hybrid films [29, 34]. The Table. 1 gives a detailed account of the RGO field emission research.

Table 1: Previous work on RGO field emission.

Morphology	**Reduction method**	**Substrate**	**Turn on field (V/μm)**	**Maximum Current density (mA/cm^2)**	**β**	**Ref.**
RGO drop casted on polystyrene film	Ultra sonication in presence of Zinc	Polystyrene	0.6	200	5818	(27)
RGO on Cu grid	Hydrazine vapour + 200^oC annealing	Cu grid	2	2	7300	(28)
RGO/CNT hybrid drop casted on Si substrate	Hydrazine dip reduction	Si	2.5	5	3976	(29)
Rgo-P3HT composite by drop casting	Hydrazine vapour	Conducting substrate	0.9 →2.9	40	1900	(30)
RGO on Ti coated Si	Thermal	Ti coated Si	4.5	~	~	(31)
RGO on ITO	Hydrazine	ITO glass	2.3	23	3700	(33)
Phenyl isocyanate factionalized RGO and polystyrene spin coating	Hydrazine + Thermal 2000 C	glass	4.7	1	1500	(34)
RGO-polyaniline composite	Hydrazine	Carbon tape	3.91	0.5	5227	(36)
composite of WS2-RGO by low-temperature hydrothermal method	In-situ hydrothermal reduction	Cu	2	0.8	2978	(37)

3. Materials and Methods

The present research aims at analysing the field emission response of RGO synthesized via EPD of aqueous solution of graphene oxide onto conducting substrate (copper). Fig. 3 represents the plan of work for the present study.

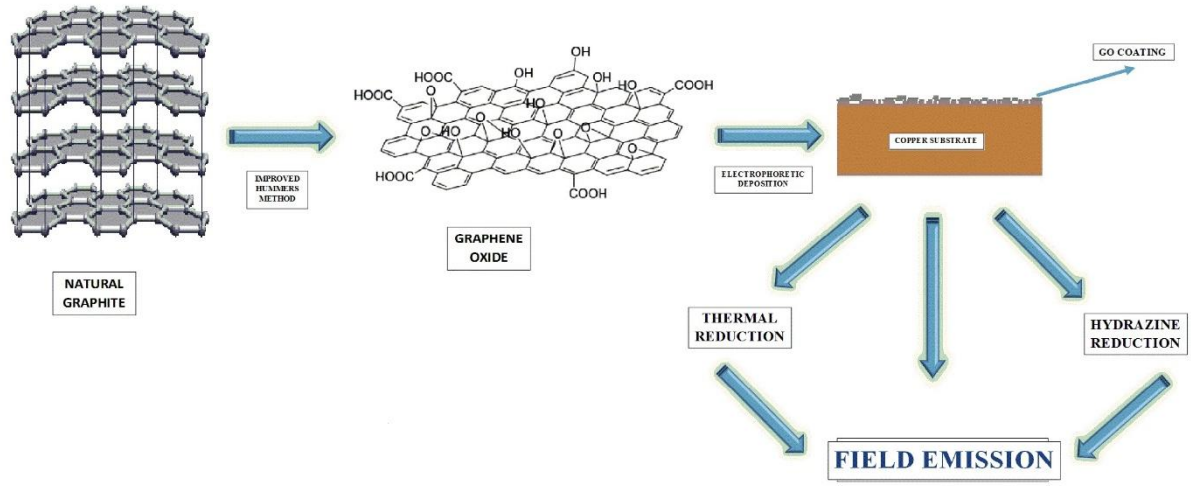

Fig. 6: Schematic representing the plan of work of the present study.

3.1. Materials and chemicals used

The following materials and chemicals have been used for the synthesis of graphene oxide to be used for EPD. All these chemicals used were of analytical grade and de-ionized water was used in all experiments in order to prevent any undesirable reactions.

Table 2: Materials and chemicals used.

Chemical	Molecular Weight (gm/mole)	Min. assay (%)	Company
Graphite	NA	99.5	
Copper sheet	63.546	99.99	Industrial grade
$KMnO_4$	158.04	99	s-d fine-chem. limited(sdfcl)
NaOH pellets	40	98	sdfcl
H_2SO_4	98.08	98	sdfcl
H_3PO_4	98	88	sdfcl
HCl	36.46	35.4	sdfcl

H_2O_2	34.01	30	sdfcl
Hydrazine monohydrate	50.06	99	
Acetone	58.08	99	sdfcl

3.2. Synthesis of graphene oxide

GO was synthesized using natural graphite flakes, ≤ 100μm in size. Graphene oxide was prepared according to modified Hummers method [38] involving oxidation of graphite flakes followed by ultra sonication to achieve graphene oxide. The method offers a single container method to synthesis of graphene oxide and requires no external temperature control. The oxidation solution containing 320ml H_2SO_4 (98.08%) and 80 ml H_3PO_4 (75%). The resultant solution was kept on magnetic stirrer and 3.2gm of graphite flakes powder was added to it at once resulting in slight increase in the temperature of the solution. Further 18gm of KMnO4 was added gradually. KMnO4 is added slowly in order to prevent extensive heating of the solution. This step should performed under a fume hood due to the release of irritating and supposedly toxic purple fumes. The resultant solution has to be kept on the magnetic stirrer for 72 hours (3 days). In this reaction, h2so4 provides oxidizing environment whereas KMnO4 acts as the oxidizing agent. The addition of H3PO4 ensures the effective oxidization of graphite basal planes whilst keeping the graphitic sp^2 structure intact. This ensures the retention of graphitic structure post reduction of the as prepared graphene oxide. The effective oxidation also renders the graphene oxide highly hydrophilic forming well dispersed aqueous solution and increases the reaction yield [41]. After 3 days of reaction 40ml of 30% H2O2 was added to the solution. The H2O2 acts as a reducing agent, reducing the left over KMnO4 in the mixture. Right after this reaction the resultant solution was dilute with lukewarm water to a total of 800ml. The precipitate so formed was washed repeatedly with de-ionized water to remove the oxidants. The next step involves washing the precipitate with 10% HCl solution in order to remove the excess metal ions generated during the oxidation process. This is followed by repeated washing with DI water till the pH of the solution becomes 4-5. The pH of the solution is then increased to about 7-8 added by adding 1M NaOH solution in order to make the graphite oxide hydrophilic and ready for mechanical exfoliation. Mechanical exfoliation is carried out using probe ultra sonication at 650 Watt for 90 minutes. Ultra sonication results in

the exfoliation of graphite oxide into graphene oxide. The resultant graphene oxide solution is well dispersed due to the presence of ionized oxygen functional groups on the sheet edges (carboxylic and hydroxyl) and shows no sign of precipitation.

3.3. Electrophoretic deposition of graphene oxide

Electrophoretic deposition (EPD) refers to deposition of charged particles onto conducting substrate under the influence of electrostatic force. Charged particles in suitable media are attracted towards oppositely charged electrode in an electric field. Charged particles lose their charge at electrodes and adhere uniformly to the surface [10].

EPD stands advantageous for thin film deposition as compared to other methods due to economical setup, easy scalability, easy parameter control and uniform deposition. Fig. 7 shows the basic mechanism of EPD in which charged particles move towards oppositely charged electrodes.

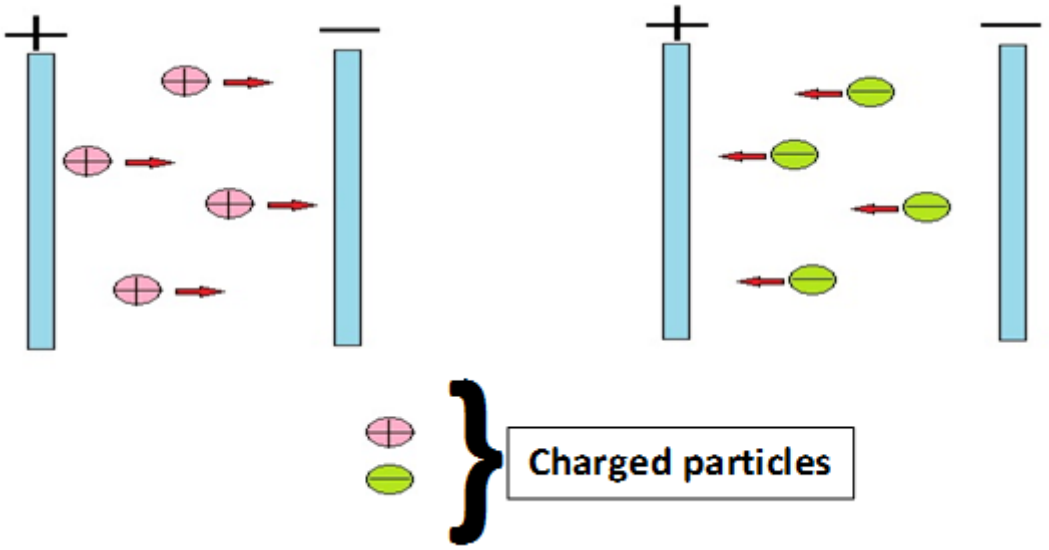

Fig. 7: Mechanism of electrophoretic deposition.

EPD has been consistently used for deposition of graphene related material onto conducting substrates for various applications such as electrodes for solar cells, field emission electrodes etc.. RGO exhibits high rate of deposition as compared to pristine graphene due to residual oxygen functional groups which are not completely eliminated during reduction.

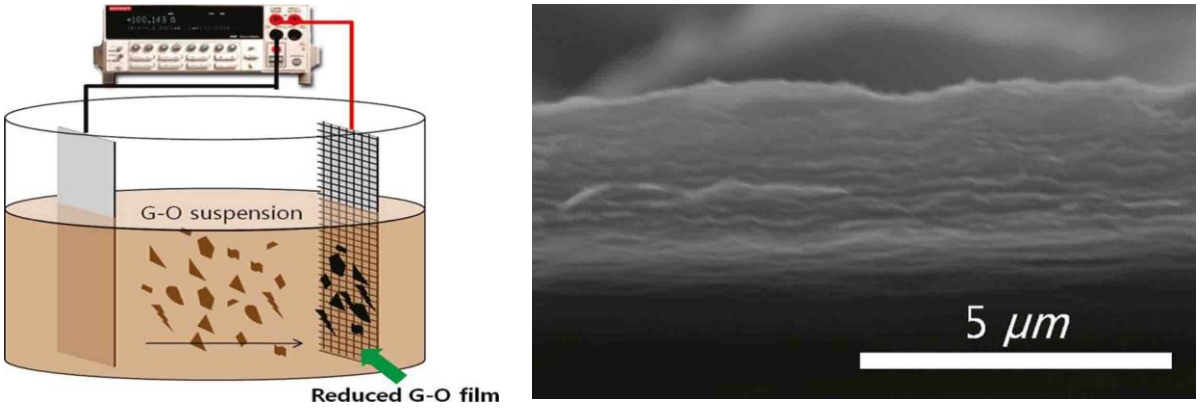

Fig. 8: Schematic diagram of the EPD process and (b) cross-sectional SEM image of EPD-GO film [15].

In the present work electrophoretic deposition of aqueous solution of GO was done on polished substrates of cold rolled copper (99.96%) 0.25 mm in thickness. Deposition was done using three different solutions with weight concentration of 0.025, 0.025 and 0.125mg/ml in DI water. Electrode gap was maintained at 5mm and voltages were fixed at 10, 15 and 20V using a low voltage DC voltage supply (0-20V). In total 9 samples were prepared using copper substrate of dimension 20X20mm. An *et. al.* confirmed the in-situ reduction of graphene oxide during electrophoretic deposition. The aim of this study is to optimize the EPD parameters such as voltage and solution concentration to develop a single step method to synthesize RGO thin films on conducting substrates. Additionally the field emission response and its dependence on the various EPD parameters was studied. The solution concentration used in our study was taken much lower as compared to Ref. [15] (1.5mg/ml). This was done in order to decrease the thickness of the as prepared films. Higher thickness RGO films showed lower substrate adhesion which may be attributed to the high cohesive energy of RGO flakes.

3.4. Subsequent reduction of RGO films

Subsequent reduction of the as prepared EPD RGO films was carried out. The intension of this step was to further reduce the RGO films and attain better electrical properties. Two methods were used separately used for the reduction:

Thermal reduction: the as prepared EPD sample were annealed at 200^{o}C for 120 minutes in Ar/H_2 (1:1) atmosphere [24]. Argon provides inert atmosphere whereas hydrogen prevents the reverse oxidation of graphene by the released gases during reduction [17]. Reduction of

graphene oxide at temperature of up to 900^0C can help in achieving complete reduction but this is not preferable as it may lead to decreased film adhesion.

Hydrazine vapour reduction: the as prepared EPD samples were maintained at 40^0C in the presence of hydrazine hydrate vapour in a parafilm sealed glass setup for 22 hr. [26].

The above reduction steps were performed for freshly prepared EPD samples and the resultant samples were tested for improvement in field emission response. In the subsequent research the as prepared EPD samples will be referred as **E-GO**, the thermally annealed samples will be referred as **ET-GO** and hydrazine treated samples will be referred as **EH-GO**

3.5. Field emission setup

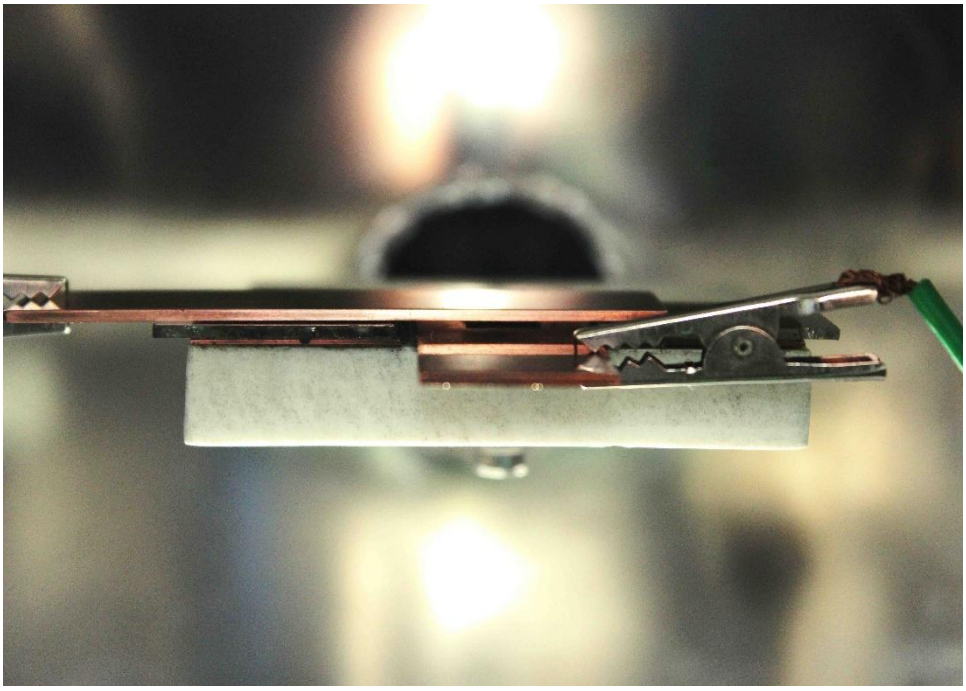

Fig. 9: Parallel plate electrode setup for field emission, upper electrode acts as anode.

In the present study field emission tests were carried out for the EPD coated metal substrates using a high vacuum chamber with average vacuum level of ~10^{-7} mbar. High voltage source PS350 (50-5000V) from Stanford Research Systems.inc was used for the field emission tests. The electrode gap was maintained at 650μm and copper was used as the counter electrode. Initially two to three power cycles, meaning voltage cycles have to be performed in order to stabilise the emission current. The turn on current was set at 10μA/cm^2. E-J characteristics were plotted for all samples till trip voltage followed by current stability test for 60-70 min.

3.6. Characterization of reduced graphene oxide

3.6.1. Field emission scanning electron microscopy

To examine the surface morphology of the reduced graphene oxide field emission scanning electron microscope (FESEM) (ULTRA plus, Carl Ziess) was used at an accelerating voltage of 15kV. Graphene and graphene oxide possess sheet like structure resulting in insufficient surface contrast in FESEM images. Owing to this graphene can only be recognized in regions of sheet overlap or sheet curling as ripples. Images were captured at varying magnifications in order to understand the variation in the RGO film morphology for different EPD parameters. Energy dispersive X-ray spectroscopy was also done for the chemical analysis of RGO films.

3.6.2. Raman spectroscopy

Raman spectroscopy is a chemical analysis technique working on the principle of inelastic scattering of visible radiation (530 nm) by various chemical species due to electronic excitations. The change in the wavelength of the incident radiation upon scattering, also called Raman shift gives the information regarding the chemical structure of the material under consideration. It very useful technique in the analysis of graphene and related structures as it can easily detect $\boldsymbol{\pi}$–$\boldsymbol{\pi}^*$ and $\mathbf{n}$–$\boldsymbol{\pi}^*$ transitions present in sp^2 and dd carbons [44]. Raman spectrum of these structures is mainly represented by three bands namely D-band, G-band and 2D-band. The D-band commonly called diamond peak is originally found at a Raman shift of 1332 cm^{-1} for crystalline diamond and represents sp^3 carbon. In case of pristine graphene this band represents the breathing mode of aromatic carbon rings (1350 cm^{-1}) and requires the presence of defects for its activation [45]. The G-band represents the E_{2g} phonon stretching of sp^2 carbon and is located around 1587 cm^{-1}. The 2D-band is the overtone of the D-band (2680cm^{-1}) i.e. low intensity second excited vibrational state [44].

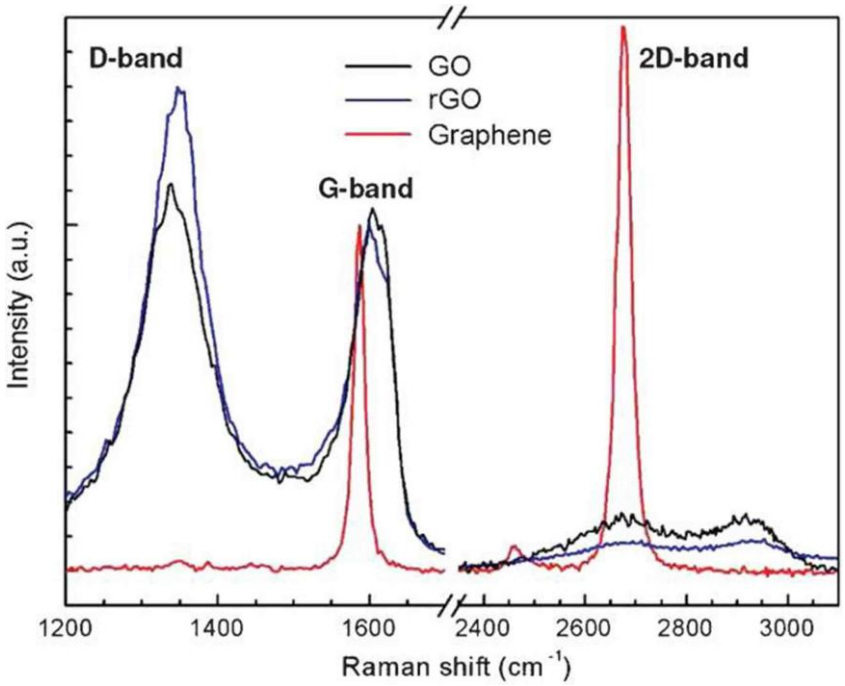

Fig. 10: Typical Raman spectra of a monolayer of GO, rGO, and mechanically exfoliated graphene on SiO_2/Si substrates [45].

The intensities of these bands (I) and their ratios also play an important role in understanding the structural characteristics of graphene. In case of graphene oxide the G-peak shifts towards higher wavenumber (1600 cm^{-1}) depicting the reduction in the size of graphitic domains [46]. The D-peak is now prominent due to the introduction of sp^3 functional groups. The intensity of the 2D-peak diminishes due to the disparity from graphitic structure. A number of studies have reported the transition of these peaks upon reduction of graphene oxide. The D-peak increases in intensity depicting the increase in degree of disorder whereas the G-peak decreases in intensity due to loss in carbon during reduction. This results in increase of I_d/I_g ratio from GO to RGO. The G and D peak undergo blue shift to lower wavenumbers. Upon reduction the intensity of the 2D peak increases and it undergoes redshift to higher wavenumber [47]. Thus the I_{2D}/I_G ratio should decrease during reduction. In conclusion the positions of these three bands and their intensity ratios can be used to characterize the extent of reduction.

In the present study Raman spectra was taken for all E-GO film samples were scanned in the range of 100cm_{-1} to 3500cm_{-1} using He-Ne laser excitation of 532nm wavelength whereas the the 0.05mg/ml 10V ET-GO and EH-GO samples were in order to characterize the extent of reduction upon deposition.

3.6.3. Fourier Transform Infrared Spectroscopy (FT-IR)

FT-IR spectroscopy works on the principle of covalent bond excitation by infra-red spectrum. The excitation frequency depends on the nature of the covalent bonds and the mass of the involved elements. The incident radiation is absorbed at vibration frequencies of various bonds and thus gives recognizable peaks. It is distinctly different from energy dispersive spectroscopy which uses monochromatic excitation source. FT-IR uses a wide spectrum of IR radiation to excite the material under test and Fourier transformation is used to compile the raw data obtained at different frequencies into one single curve. The possibility to detect the various organic bonds such as C=O (1720cm-1), C-OH (1220cm-1), C-O (1060cm-1), sp^2 carbon (1600cm-1) and O-H (3400cm-1) makes FT-IR a suitable tool for the study of chemical structure of GO and RGO [48]. The variation in the spatial density of these functional groups can be identified from the extent of absorption at the above mentioned peaks.

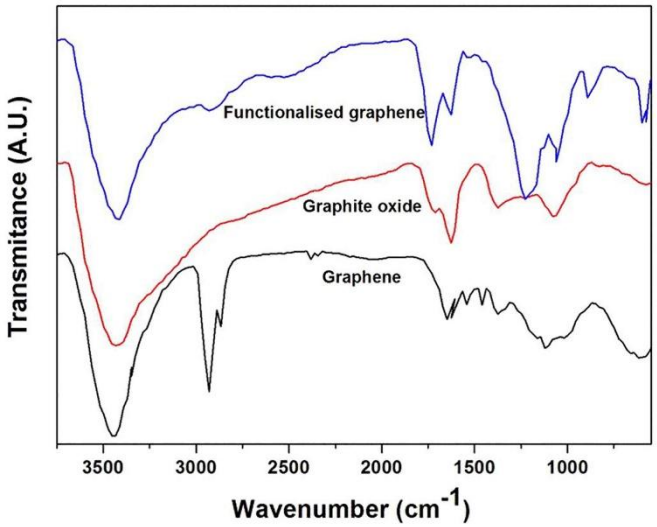

Fig. 11: Typical FTIR spectra of graphene, thermally reduced graphite oxide and functionalised graphene. [49]

In the present study FT-IR spectra of the prepared E-GO films was carried out using Nicolet AVATAR 360 FTIR spectrometer with a Smart OMNI Sampler with a germanium crystal. The aim of this characterization was to detect the removal of different oxygen functional groups from GO upon EPD deposition and its dependence on EPD parameters.

3.6.4. Ultra-Violet Visible absorption spectroscopy

UV-visible spectroscopy refers to the absorbance spectrum of a material under the incidence of UV to near-IR radiation. The material under consideration undergo characteristic electronic transitions depending on the bonds present. The common electronic transitions include $\pi \rightarrow \pi^*$ and $n \rightarrow \pi^*$. In case of well oxidized graphene oxide the UV peak is located at ~230nm wavelength attributable to $\pi \rightarrow \pi^*$ transition [45]. Upon reduction the peak undergoes red shift up to a maximum of 275nm. This shift can be attributed to the increase in the sp^2 bonded carbon species and the reduction in the band gap of graphene upon removal of oxygen functional groups. Also, in case of RGO the absorbance peak has lower intensity. Smaller graphitic domains and defects introduced during reduction are the likely causes for this phenomenon [48]. A distinct shoulder is formed in the absorption spectra of GO at 300nm depicting the $n \rightarrow \pi^*$ transition of C=O [45].

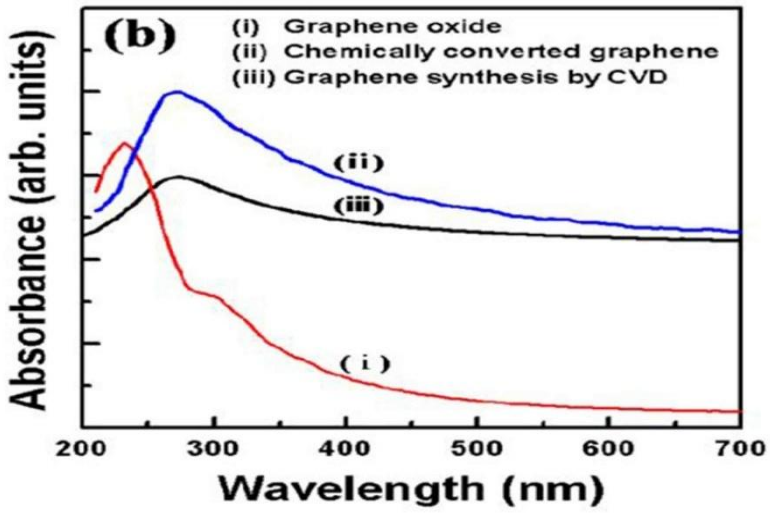

Fig. 12: Typical absorbance spectra in UV to visible wavelength region of (i) graphene-oxide, (ii) chemically converted graphene (CCG), and (iii) graphene (MLG) films synthesized by CVD.

In the present study, UV spectra was taken for as prepared GO (0.03mg/ml) and the E-GO (0.01mg/ml) with the objective of analysing the red shift of UV peak for the E-GO samples upon reduction.

3.6.5. X-Ray Diffraction (XRD)

XRD technique works on the principle of constructive interference of electromagnetic rays (0.01-1000nm) diffracted by crystalline material. It is used to characterize the crystal structure, presence of various phases and elemental composition. In case of graphene, GO and RGO XRD provides information about the d-spacing of graphene basal planes and thus the extent of reduction. The 2θ position is found for graphene at 26.5^0 (0.333nm), graphene oxide at 10^0 (0.860nm) and for RGO from 13.24^0 to 26.05^0 (0.668 to 0.342nm) [47]. Fig. 13 shows typical XRD curves for

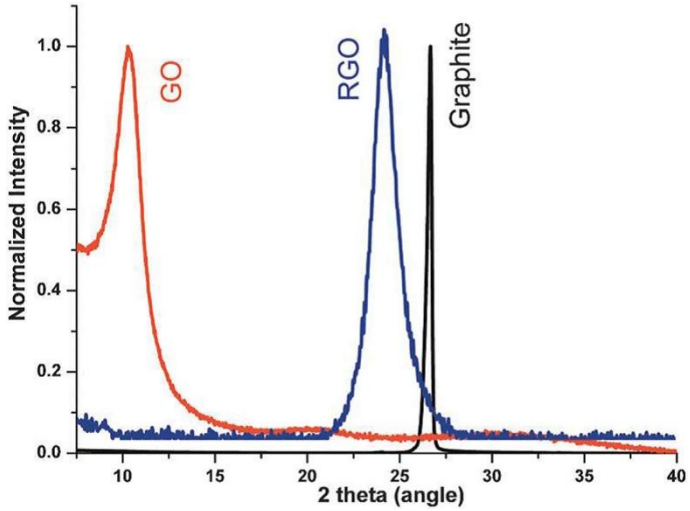

Fig. 13: Typical powder XRD pattern of graphite (black), GO (red) and rGO (blue) [50].

4. Results and Discussion

4.1. Structural and chemical analysis

4.1.1. FE-SEM

FE-SEM analysis was carried out for the E-GO samples at varying magnifications was done and a comparison of the images taken at 50X magnification is as shown in fig. 14. As RGO possesses sheet like structure the relative contrast between different areas is very low. Presence of RGO sheets can only be realized in regions of sheet overlap or sheet ripples.

More sheet edges were visible as we moved to samples with higher EPD voltage and higher deposition solution concentrations. At lower concentrations the RGO sheets adhere parallel to the surface of the substrate (Cu). But as the voltage and concentration increases the number of sheets being deposited increases. After the initial sheets adhere parallel to the substrate the simultaneously deposited sheets may adhere to the substrate or the interface of previously deposited RGO and the substrate. This results in the RGO sheet having an angular morphology with respect to the substrate. The result of this is higher film roughness. The random orientation of the RGO sheets may favour better Field emission characteristics due to the higher field enhancement factor.

The EDX analysis of the as prepared E-GO films gives some insight into the thickness of the as prepared films and the resultant C/O ratio. The C/O ratio increased from below 2 on as prepared GO to 3.89 in case of E-GO. The comparison of the EDX data for 0.05mg/ml E-GO samples is shown in table 3.

Table 3: EDX analysis for 0.05mg/ml E-GO samples .

GO SOLUTION	DEPOSITION VOLTAGE	ATOMIC % (EDX)			C/O RATIO
		CARBON	OXYGEN	COPPER	
0.05	10	42.42	14.43	43.14	2.93
0.05	15	65.61	16.87	17.51	3.89
0.05	20	60.71	25.53	13.76	2.38

a) 0.025mg/ml

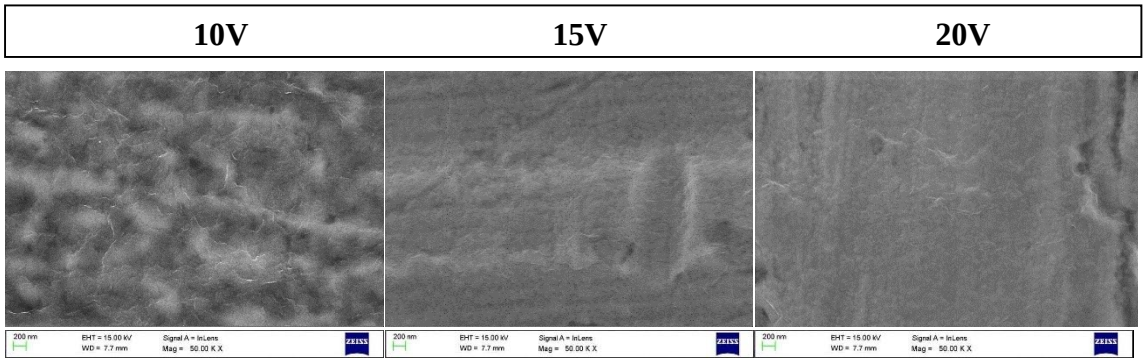

b) 0.05mg/ml

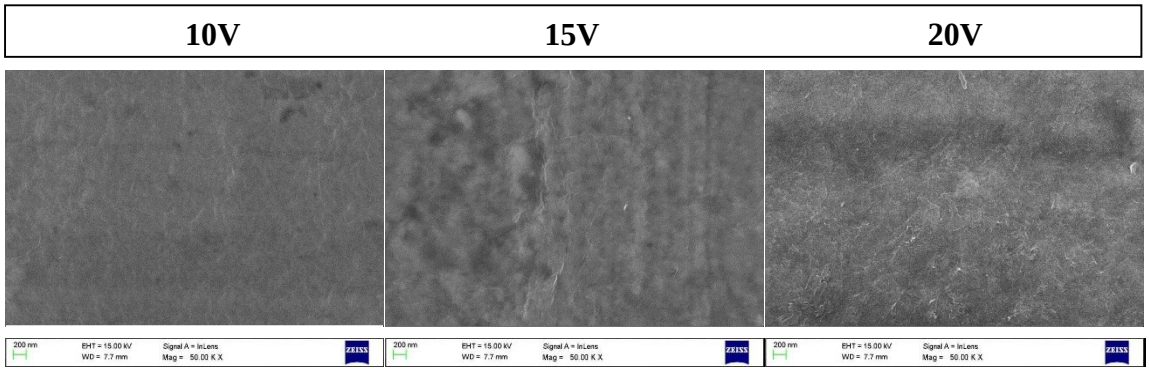

c) 0.125mg/ml

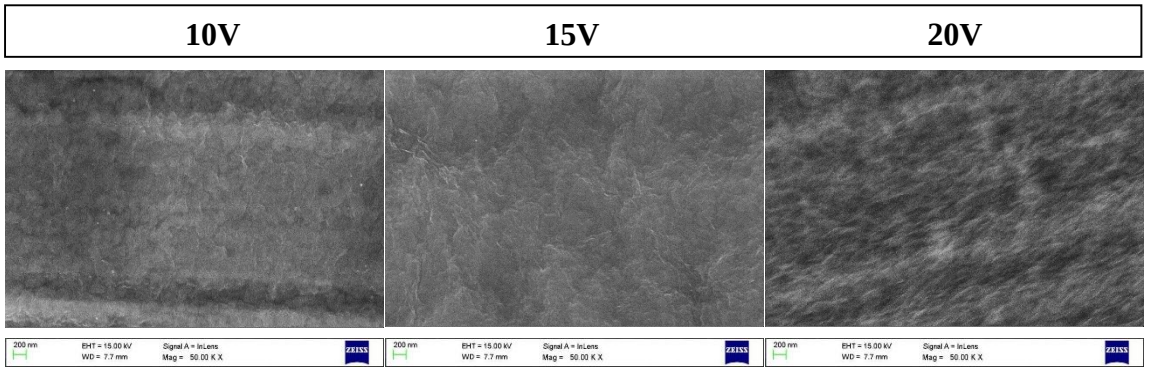

Fig. 14: FE-SEM images for E-GO samples.

4.1.2. XRD analysis

XRD analysis was done for as prepared GO and RGO reduced using thermal annealing (T-GO) and hydrazine vapour (H-GO) in powder form. Fig. 15 shows the comparison between the XRD pattern for GO, H-GO and T-GO. The (002) peak for GO indicates augmented d-spacing between the graphite basal planes due to the intercalated oxygen functional groups like hydroxyl, carboxylic and carbonyl. The d-spacing increased from 3.3 Å for pristine graphite to 8.58 Å for GO powder. The (002) peaks for both T-GO and H-GO powder indicate the regain of graphitic structure by shift in the XRD peak towards that of graphite (2θ~26.4°).

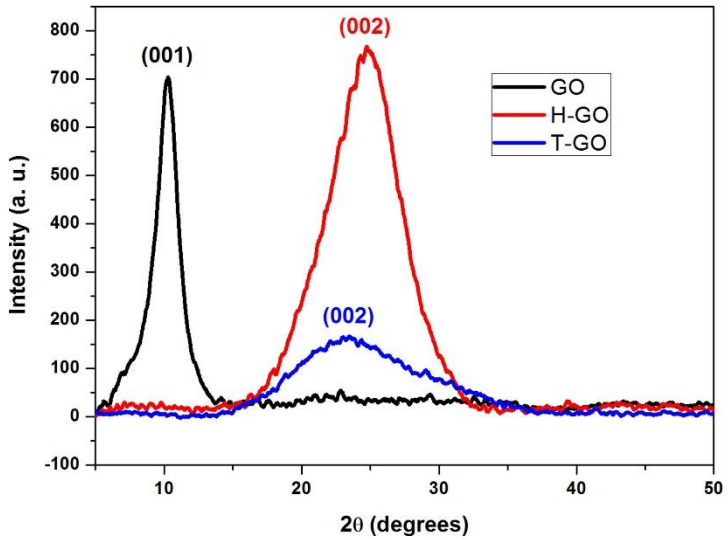

Fig. 15: XRD pattern for GO, H-GO and T-GO powder.

The peak position indicate better reduction in the case of H-GO, with the diffraction peak being closer to that of graphite and minor increase in the FWHM. In case of T-GO the FWHM was seen to increase drastically which might be as a result of the higher deterioration of the sp^2 structure of the GO and the reduction in the size of the particles upon reduction. Table. 4 gives the comparison between the (002) peak XRD data for GO, T-GO and H-GO.

Table 4: Comparison of XRD data for GO, H-GO and T-GO powder.

Sample	**2θ (degrees)**	**d – spacing (Å)**	**FWHM (degrees)**
GO	10.3	8.58	1.915
H-GO	24.72	3.6	6.149
T-GO	23.42	3.79	10.617

4.1.3. UV analysis

UV visible spectroscopy was carried out for the GO solution to confirm the proper oxidation of the graphite. Literature data reports the UV peak position between 230nm. The peak for the GO solution was found to be at 235 nm. Fig. 16 shows the UV-visible absorption spectra for GO aqueous solution.

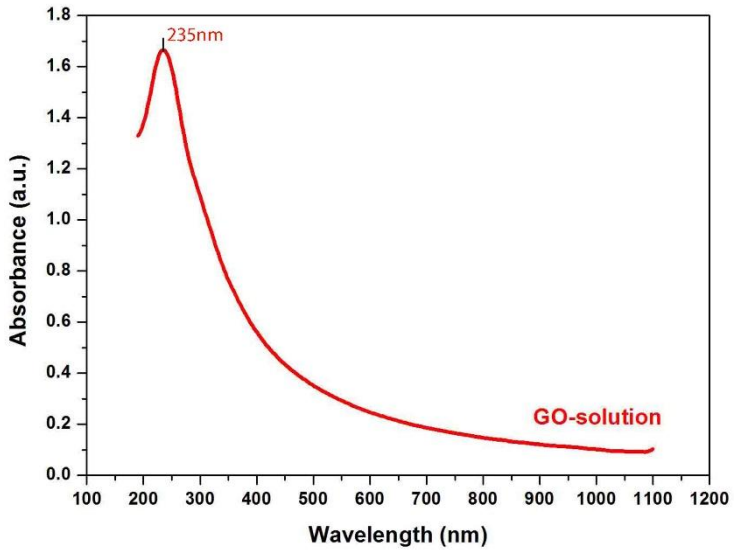

Fig. 16: UV-visible absorption spectra for GO aqueous solution.

4.1.4. Raman analysis

Raman spectroscopy was carried out for the as prepared GO solution as well as the E-GO samples in order to analyse the reduction of GO upon EPD and its dependence on the EPD parameters. Table. 5 shows the comparison of the Raman data obtained from these samples. The intensity of both G and D peaks reduced considerably from the GO sample to the E-GO samples and at the same time peak positions for both these peaks showed considerable red shift upon deposition. As mentioned in the section. 3.6.2, both these phenomenon indicate the reduction of GO. Thus both D and G peak were seen approaching the peak positions of pristine graphene *i.e.* 1348cm^{-1} and 1587cm^{-1} for the D and the G peak respectively. This confirms the reduction of GO upon EPD. During reduction of GO both I_d and I_g decrease but the decrease in I_g is relatively more as compared I_d. This may be attributed to the decrease in the average sp^2 domain size either by the random removal of functional groups or by the nucleation of new sp^2 domains as explained in the section 3.6.2. This results in the increase in the I_d/I_g ratio upon reduction.

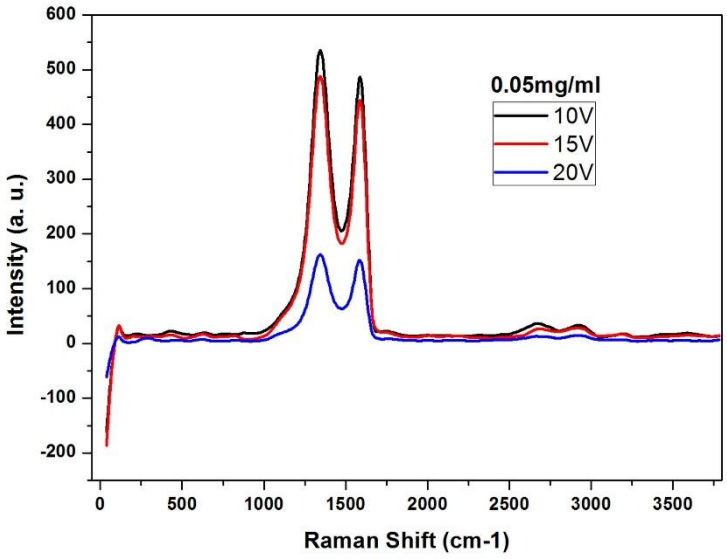

Fig. 17: Raman shift for 0.05mg/ml E-GO samples.

From the table. 5 it is clear that the I_d/I_g ratio increased for all the E-GO samples. Also the ratio showed an increasing pattern with the increase in the EPD voltage and the solution concentration.

Table 5: Comparison of Raman data for E-GO samples.

sample	solution	voltage	D band (cm^{-1})	G band (cm^{-1})	I_d/I_g
E-GO	0.025	10V	1352.37	1599.44	1.14
E-GO	0.025	15V	1348.38	1599.44	1.103
E-GO	0.025	20V	1348.38	1599.44	1.167
E-GO	0.05	10V	1348.38	1587.84	1.165
E-GO	0.05	15V	1348.38	1587.84	1.28
E-GO	0.05	20V	1348.38	1591.71	1.26
E-GO	0.125	10V	1352.37	1599.44	1.25
E-GO	0.125	15V	1348.38	1599.44	1.303
E-GO	0.125	20V	1348.38	1587.84	1.36
GO	powder	n/a	1352.08	1601.16	0.8988

In order to analyse the reduction of the EPD samples upon further treatment with hydrazine vapour and thermal treatment, Raman data was collected for the sample showing maximum current in field emission *i.e.* 0.05mg/ml EH-GO and ET-GO sample. Table 6 shows the comparison of Raman data obtained for these samples. The increase in the I_d/I_g confirms the

further reduction of the RGO. As confirmed by previous research works the ratio increase was more for hydrazine vapour treatment was more as compared to the thermal reduction. Also, a peak shift was observed in the peak position of the 2D peak. This confirms the further reduction of the RGO as mentioned in the section 3.6.2.

Table 6: Comparison of Raman data for 0.05mg/ml, 10V; E-GO, ET-GO and EH-GO samples.

sample	reduction	D band	G band	2D band	I_d/I_g
E-GO	EPD	1348	1588.8	2680.86	1.165
ET-GO	Thermal	1348	1587.8	2702.94	1.18642842
EH-GO	Hydrazine vapour	1348	1588	2764.46	1.24743331

4.2. Field emission analysis

4.2.1. Field emission response

Field emission tests were conducted for all samples of E-GO, EH-GO and ET-GO was conducted. A maximum emission current of 2.7 mA/cm^2, lowest turn on field of 1.5 v/µm and highest field enhancement factor of 6404 was achieved. The emission response behaviour of the samples show marked dependence on the various EPD parameters as well as the simultaneous reduction of the E-GO samples. Table. 7 gives the comparison of the field emission response of from the E-GO samples.

For the E-GO samples the 0.05mg/ml samples showed the best field emission results. The field emission response of any type of emitters depends on the aspect ratio of the emitters, the spatial distribution and the adhesion with the substrate. The field emission current in the 0.025mg/ml samples was comparatively low. The film prepared from 0.025mg/ml GO solution had a very thin coating well adhered to the substrate. This results in the RGO sheets lying parallel to the substrate and offering very low aspect ratio. The field emission again was found to be low for the 0.125mg/ml samples. This may again be explained with the help of the sheet morphology. The films prepared from the 0.125mg/ml solution were much thicker and had a very low adhesion with the substrate, which might be traced back to the fact that the cohesion of RGO

is higher as compared to its adhesion with the substrate as explained in the previous sections. This leads to the detachment of the emitters during field emission test. Figure 18 shows the current density plot and the corresponding F-N plot for the 0.05mg/ml E-GO samples.

Table 7: Field emission response for E-GO samples.

Sl. No.	Solution concentration (mg/ml)	EPD voltage (Volts)	Turn on field (V/µm)	Maximum current (mA/cm^2)	Field enhancement factor (β)
1	0.025	10	3.08	0.4	1533
2	0.025	15	2.23	0.28	2194
3	0.025	20	1.77	0.6	2098
4	0.05	10	3	2.08	1919
5	0.05	15	2.23	2	6776
6	0.05	20	1.77	1.4	4431
7	0.125	10	3.23	1.2	2440
8	0.125	15	3.15	0.6	3430
9	0.125	20	3.08	0.48	2786

Field emission tests were also conducted for the EH-GO and the ET-GO samples. Both the set of samples showed higher emission current and lower turn on fields as compared to the as prepared E-GO samples. The emission current was found to be maximum in the EH-GO samples .this might be attributed to the fact that hydrazine results in a better regain of the conductivity of the RGO sheets, as confirmed by the previous research work. Table 8 compares the field emission response for the EH-GO samples.

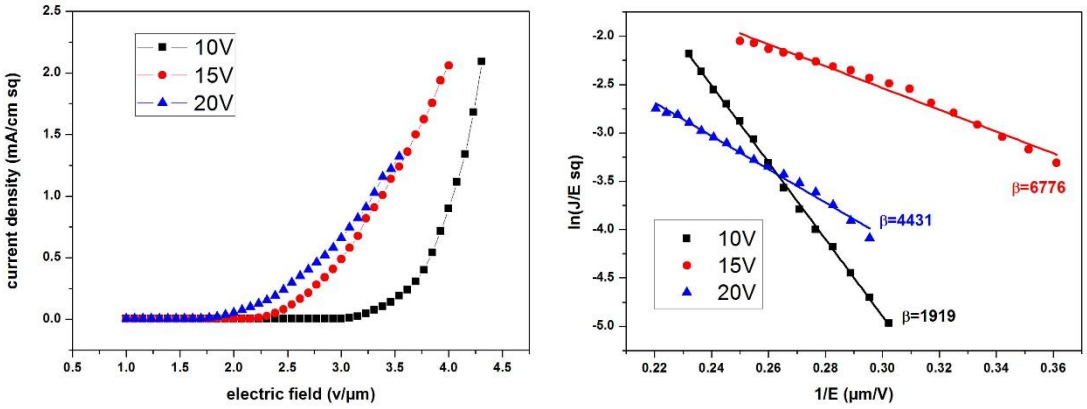

Fig. 18: a) current density plot, and b) F-N plot, for 0.05mg/ml for E-GO samples.

Table 8: Field emission response for EH-GO samples.

Sl. No.	Solution concentration (mg/ml)	EPD voltage (Volts)	Turn on field (V/µm)	Maximum current (mA/cm^2)	Field enhancement factor (β)
1	0.025	10	2.7	0.96	3738
2	0.025	15	2.15	0.82	1940
3	0.025	20	1.7	1.042	2979
4	0.05	10	2.7	2.72	2247
5	0.05	15	2.1	2.21	3609
6	0.05	20	1.62	1.8	4233
7	0.125	10	2.8	1.84	2237
8	0.125	15	2.62	1.64	2332
9	0.125	20	2.55	0.94	2217

Again the same emission behaviour was followed by the E-GO samples with the 0.05mg/ml samples showing highest emission currents and the lowest turn fields. Figure 19 gives the current density plot and the F-N plot for the EH-GO samples. Marked improvement was also seen in the field enhancement factor of the samples after reduction. The change in the morphology of the films upon further reduction may be the reason behind this improvement.

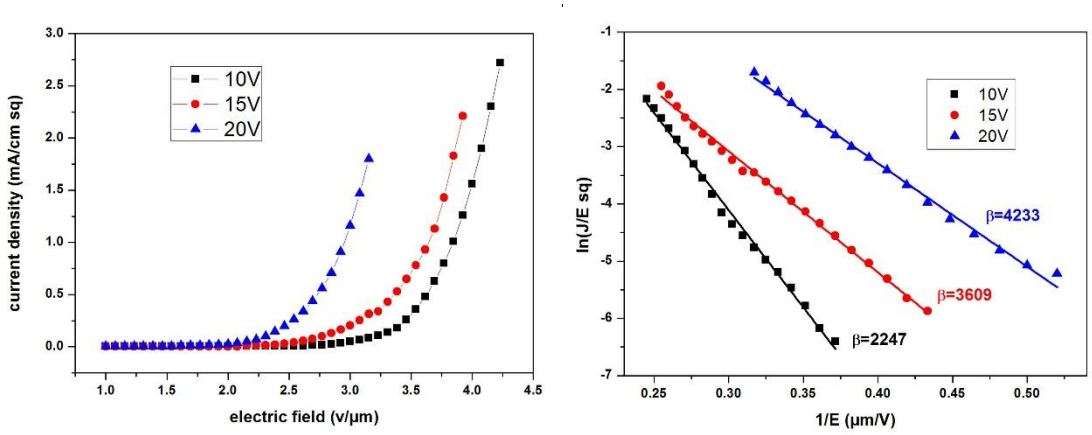

Fig. 19: a) current density plot, and b) F-N plot, for 0.05mg/ml EH-GO samples.

The lowest turn on field among all the samples was exhibited by the ET-GO samples. This indicates towards the fact that these samples possess the lowest band gap among all the three sets of the samples. This fact is also confirmed by earlier works. The thermal reduction results in the effective lowering of the band gap of the GO. Table 9 compares the field emission response for the ET-GO samples.

Table 9: Field emission response for ET-GO samples.

Sl. No.	Solution concentration (mg/ml)	EPD voltage (Volts)	Turn on field (V/µm)	Maximum current (mA/cm^2)	Field enhancement factor (β)
1	0.025	10	2.45	0.84	2900
2	0.025	15	2	0.74	4631
3	0.025	20	1.65	1.1	4833
4	0.05	10	2.5	2.61	2591
5	0.05	15	1.81	2.06	4095
6	0.05	20	1.5	1.68	7006
7	0.125	10	2.5	1.86	2805
8	0.125	15	2.45	1.18	2411
9	0.125	20	2.4	0.8	2654

The lowest turn on field of 1.5V/µm was achieved for the ET-GO samples. Field enhancement factors as high as 6404 were achieved with these samples. As in the results of E-GO and EH-GO the best field emission response was shown by the 0.05mg/ml samples. Figure 20 gives the current density plot and the F-N plot for the 0.05mg/ml ET-GO samples.

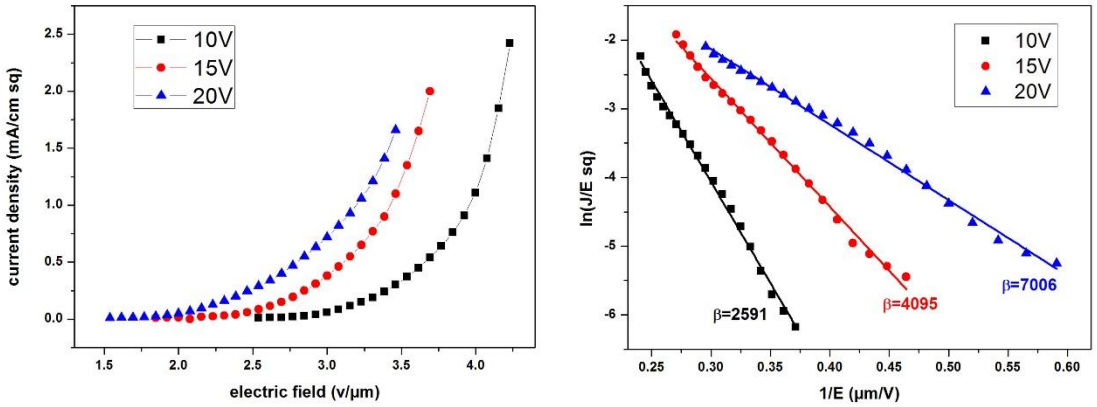

Fig. 20: a) current density plot, and b) F-N plot, for 0.05mg/ml ET-GO samples.

4.2.2 Stability test

Stability test was conducted for the E-GO samples at 30% of the maximum emission current density for about 70 min. A maximum fluctuation of 32.8, 80 and 65 percent was recorded for the 10V, 15V and the 20V samples respectively. Fig. 21 shows the current stability plots for the 0.05mg/ml samples.

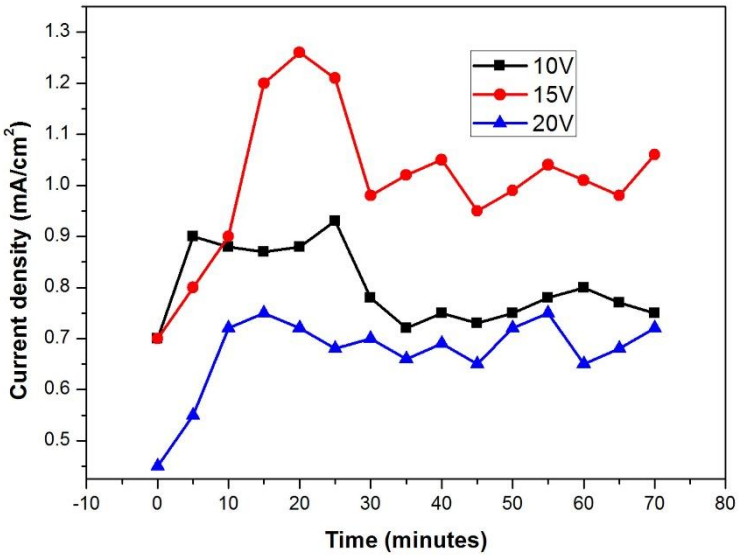

Fig. 21: current stability plot for 0.05mg/ml samples taken at ~30% of maximum emission current.

4.2.3. Comparison with literature data

Table 10: comparison of current field emission data with similar prior research.

Sample	Turn on field (V/μm)	Maximum current (mA/cm^2)	Field enhancement factor (β)	Ref.
RGO on Cu grid (hydrazine + thermal reduction)	2	2	7300	(28)
RGO/CNT hybrid drop casted on Si substrate (hydrazine dip reduction)	2.5	5	3976	(29)
E-GO 0.05mg/ml 10V	3	2.08	1919	Present study
E-GO 0.05mg/ml 15V	2.23	2	6776	Present study
ET-GO 0.05mg/ml 20V	1.5	1.68	7006	Present study
EH-GO 0.05mg/ml 10V	2.7	2.72	2247	Present study

4.2.3. Potential applications

Since its discovery graphene has made its appearance in a vast majority of electronic devices including field effect transistors, solar cells, supercapacitors etc. the key reasons for this are high conductivity, flexibility, atomically thin edges and optical transmittance. RGO possesses these properties and can be bulk synthesized easily. Thus, the consideration of RGO electronic devices stands inevitable. RGO has been used to prepare the counter electrodes for dye sensitized solar cells via EPD [7]. Fig. 22 shows the schematic of the setup used for the preparation of RGO counter electrodes. The reduction of the GO was carried out before EPD in the above work. The anodic reduction method mentioned in the present study can be utilized for 1 step preparation of counter electrodes.

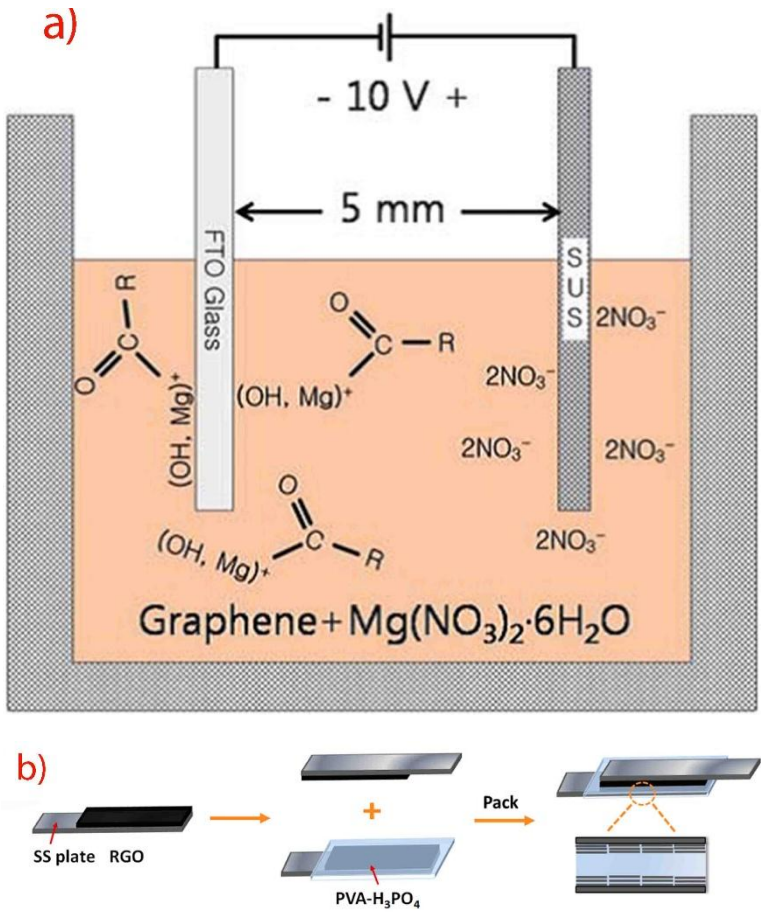

Fig. 22: Schematic for preparation of a) RGO counter electrode for dye sensitized solar cell [7] and b) RGO supercapacitor [51].

As a result of sheet like structure and atomically thin edges RGO posess a very high surface area to weight ratio. This property of RGO has been utilized to prepare supercapacitor electrodes [51]. The large surface area allows the RGO to store large amount of charge within a small area resulting in high capacitance. In the work by Wang et. al. reduced RGO was electrophoretically deposited onto stainless steel substrate in order to prepare the electrodes. The method can be improved by using 1 step anodic reduction and deposition (used in the present study) to directly prepare the electrodes. The low turn on field and high emission current for anodically reduced graphene oxide also opens up the possibility of its application for various field emission devices.

5. Conclusions

From the above results it is convincingly clear that conducting thin films of RGO can be prepared by a single step electrophoretic deposition method. The as prepared thin films are capable of enhanced field emission which was dependent on the film morphology and thickness. The method proves highly efficient as most of the previous research work involved reduction of graphene oxide before deposition onto substrates. The RGO film thickness was seen to increase with the depth of electrode in the EPD solution. This phenomena needs to be further studied in order to prepare RGO films of controlled transparency, so that they can be utilized for photovoltaic applications. The actual mechanism of the anodic reduction of graphene oxide during EPD still needs to be understood and necessitates a detailed research on the method.

6. Future Scope

The present study was mainly focussed on the dependence of field emission response and reduction of RGO upon EPD anodic reduction. In order to understand the applicability of this anodically reduced graphene oxide for electronic devices further study of properties of RGO has to be carried out. The adhesion of the as prepared films with the substrate plays an important role in deciding the life and efficiency of the devices prepared from it. Thus, nanoscratch study of the various as prepared RGO films can be carried out. In case of solar cell applications the transmittance of the as prepared films is a concern. For the samples prepared in the present study the film thickness increased with increase in the EPD voltage and the solution concentration and thus the transmittance varies with these parameters. The suitable parameters for deposition can be deduced by conducting transmittance studies. The dependence of the extent of reduction of GO during EPD on the substrate used has to be carried out for better insight into the mechanism of anodic reduction.

References

[1] Yuan Huang, Weiliang Wang, Juncong She, Zhibing Li, Shaozhi Deng : Correlation between carbon–oxygen atomic ratio and field emission performance of few-layer reduced graphite oxide ; Carbon, 2012, vol. 50, pp.2657-2665.

[2] Minkyu Kim, Choonghyeon Lee, Young Deok Seo, Sunghun Cho, Jihoo Kim, Gyeongseop Lee, Yun Ki Kim and Jyongsik Jang ; Fabrication of Various Conducting Polymers Using Graphene Oxide as a Chemical Oxidant ; Chem. Mater., 2015, vol. 27, pp. 6238-6248.

[3] Georgios M. Viskadouros, Minas M. Stylianakis, Emmanuel Kymakis, and Emmanuel Stratakis : Enhanced Field Emission from Reduced Graphene Oxide Polymer Composites, ACS Appl. Mater. Interfaces, 2014, Vol. 6, pp. 388-393.

[4] Khan M. F. Shahil and Alexander A. Balandin; Graphene – Based Nanocomposites as Highly Efficient Thermal Interface Materials; Nanotechnology (IEEE-NANO) 11th IEEE Conference, 2011, pp.1193-1196.

[5] Wei Chen, R. B. Rakhi and H. N. Alshareef; Capacitance enhancement of polyaniline coated curved-graphene supercapacitors in a redox-active electrolyte; Nanoscale, 2013, Vol. 5, pp.4134-4138.

[6] Narjes Kheirabadi and Azizollah Shafiekhani; Graphene/Li-ion battery; Journal of Applied Physics, 2012, Vol. 112, pp. 124323.

[7] Hyonkwang Choi, Hyunkook Kim, Sookhyun Hwang, Youngmoon Han and Minhyon Jeon; Graphene counter electrodes for dye-sensitized solar cells prepared by electrophoretic deposition; J. Mater. Chem., 2011, Vol. 21, pp. 7548.

[8] You Min Chang, Hyungseok Kim, Ju Han Lee, and Yong-Won Song; Multilayered graphene efficiently formed by mechanical exfoliation for nonlinear saturable absorbers in fiber mode-locked lasers; Applied Physics Letters, 2010, Vol. 97, pp. 211102.

[9] G. Deokar , J. Avila , I. Razado-Colambo , J.-L. Codron , C. Boyaval , E. Galopin , M.-C. Asensio , D. Vignaud ,Towards high quality CVD graphene growth and transfer; Carbon, 2015, Vol. 8 9, pp. 82-92.

[10] Daniela C. Marcano, Dmitry V. Kosynkin, Jacob M. Berlin, Alexander Sinitskii, Zhengzong Sun, Alexander Slesarev, Lawrence B. Alemany, Wei Lu, and James M. Tour; Improved Synthesis of Graphene Oxide; ACS Nano, 2010, Vol. 4, No. 8, pp. 4806-4814.

[11] Mahmoud Nasrollahzadeh, Ferydon Babaei, Parisa Fakhric and Babak Jaleh; Synthesis, characterization, structural, optical properties and catalytic activity of reduced graphene oxide/copper nanocomposites; RSC Adv., 2015, Vol. 5, pp. 10782-10789.

[12] Chun Kiang Chua and Martin Pumera; Chemical reduction of graphene oxide: a synthetic chemistry viewpoint; Chem. Soc. Rev., 2014, Vol. 43, pp. 291-312.

[13] Yuyan Shao, Jun Wang, Mark Engelhard, Chongmin Wang and Yuehe Lin; Facile and controllable electrochemical reduction of graphene oxide and its applications; J. Mater. Chem., 2010, Vol. 20, pp. 743-748.

[14] Xingfa Gao, Joonkyung Jang, and Shigeru Nagase; Hydrazine and Thermal Reduction of Graphene Oxide: Reaction Mechanisms, Product Structures, and Reaction Design; J. Phys. Chem. C, 2010, Vol. 114, No. 2, pp. 832-842.

[15] Sung Jin An, Yanwu Zhu, Sun Hwa Lee, Meryl D. Stoller, Tryggvi Emilsson, Sungjin Park, Aruna Velamakanni, Jinho An, and Rodney S. Ruoff: Thin film fabrication and simultaneous reduction of deposited graphene oxide platelets by electrophoretic deposition J. Phys. Chem. Lett., (2010), Vol. 1, pp. 1259-1263.

[16] Priyank V. Kumar, Marco Bernardi, and Jeffrey C. Grossman; The Impact of Functionalization on the Stability, Work Function, and hotoluminescence of Reduced Graphene Oxide; ACS Nano, 2013, Vol. 7, No. 2, pp. 1638-1645.

[17] Songfeng Pei, Hui-Ming Cheng; The reduction of graphene oxide; Carbon, 2012, Vol. 50, pp. 3210-3228.

[18] Laxmidhar Besra, Meilin Liu: A review on fundamentals and applications of electrophoretic deposition (EPD), Progress in Materials Science, 2007, Vol. 52, pp. 1-61.

[19] Zhong-Shuai Wu, Songfeng Pei, Wencai Ren, Daiming Tang, Libo Gao, Bilu Liu, Feng Li, Chang Liu, and Hui-Ming Cheng : Field Emission of Single-Layer Graphene Films Prepared by Electrophoretic Deposition, Adv. Mater., 2009, Vol. 21, pp. 1756-1760.

[20] Caterina Soldano, Ather Mahmood, Erik Dujardin; Production, properties and potential of graphene; Carbon, 2010, Vol. 48, pp. 2127-2150.

[21] C. N. R. Rao, A. K. Sood, K. S. Subrahmanyam, and A. Govindaraj; Graphene: The New Two-Dimensional Nanomaterial; Angew. Chem. Int. Ed., 2009, Vol. 48, pp. 7752-7777.

[22] Sumit Saxena, Trevor A. Tyson, and Ezana Negusse; Investigation of the Local Structure of Graphene Oxide; J. Phys. Chem. Lett., 2010, Vol. 1, pp. 3433-3437.

[23] Dongxing Yanga, Aruna Velamakannia, Gu lay Bozoklub, Sungjin Parka, Meryl Stollera, Richard D. Pinera, Sasha Stankovichc, Inhwa Junga, Daniel A. Fieldd, Carl A. Ventrice Jr.d, Rodney S. Ruoffa; Chemical analysis of graphene oxide films after heat and chemical treatments by X-ray photoelectron and Micro-Raman spectroscopy; Carbon, 2009, Vol. 47, pp. 145-152.

[24] Bing Zhaoa, Peng Liua, Yong Jianga, Dengyu Pana, Haihua Taob, Jinsong Songa, Tao Fanga, Weiwen Xua; Supercapacitor performances of thermally reduced graphene oxide; Journal of Power Sources, 2012, Vol. 198, pp. 423-427.

[25] Sasha Stankovich, Dmitriy A. Dikin, Richard D. Piner, Kevin A. Kohlhaas, Alfred Kleinhammes, Yuanyuan Jia, Yue Wu, SonBinh T. Nguyen, Rodney S. Ruoff; Synthesis of graphene-based nanosheets via chemical reduction of exfoliated graphite oxide; Carbon, 2007, Vol. 45, pp. 1558-1565.

[26] Héctor A. Becerril, Jie Mao, Zunfeng Liu, Randall M. Stoltenberg, Zhenan Bao and Yongsheng Chen; Evaluation of Solution-Processed Reduced Graphene Oxide Films as Transparent conductors; ACS nano, 2008, Vol. 2, No. 3, pp. 463-470.

[27] I. Sameera, Ravi Bhatia, Jianyong Ouyang, V. Prasad, and R. Menon : Electron field emission from reduced graphene oxide on polymer film, Applied Physics Letters, 2013, Vol. 102, pp. 033102.

[28] Hisato Yamaguchi, Katsuhisa Murakami, X Goki Eda, Takeshi Fujita, Pengfei Guan, WeichaoWang, Cheng Gong, Julien Boisse, Steve Miller, Muge Acik, Kyeongjae Cho, Yves J. Chabal, Mingwei Chen, Fujio Wakaya, Mikio Takai and Manish Chhowalla; Field Emission from Atomically Thin Edges of Reduced Graphene Oxide; ACS Nano, 2011, Vol. 5, No. 6, pp. 4945-4952.

[29] Duc Dung Nguyen, Yi-Ting Lai, Nyan-Hwa Tai; Enhanced field emission properties of a reduced graphene oxide/carbon nanotube hybrid film; Diamond & Related Materials, 2014, Vol. 47, pp. 1–6.

[30] Georgios M. Viskadouros, Minas M. Stylianakis, Emmanuel Kymakis, and Emmanuel Stratakis : Enhanced Field Emission from Reduced Graphene Oxide Polymer Composites, ACS Appl. Mater. Interfaces, 2014, Vol. 6, pp. 388-393.

[31] Jun Li, Jiangtao Chen, Baomin Luo, Xingbin Yan, and Qunji Xue; The improvement of the field emission properties from graphene films: Ti transition layer and annealing process; AIP Advances, 2012, Vol. 2, pp. 022101.

[32] Dexian Ye, Sherif Moussa, Josephus D. Ferguson, Alison A. Baski, and M. Samy El-Shall ; Highly Efficient Electron Field Emission from Graphene Oxide Sheets Supported by Nickel Nanotip Arrays; Nano Lett., 2012, Vol. 12, pp. 1265-1268.

[33] Zhong-Shuai Wu, Songfeng Pei, Wencai Ren, Daiming Tang, Libo Gao, Bilu Liu, Feng Li, Chang Liu, and Hui-Ming Cheng : Field Emission of Single-Layer Graphene Films Prepared by Electrophoretic Deposition, Adv. Mater., 2009, Vol. 21, pp. 1756-1760.

[34] Goki Eda, H. Emrah Unalan, Nalin Rupesinghe, Gehan A. J. Amaratunga, and Manish Chhowalla; Field emission from graphene based composite thin films; Applied Physics Letters, 2008, Vol. 93, pp. 233502.

[35] Jianhui Dong, Baoqing Zeng, Yucheng Lan, Shikai Tian, Yun Shan, Xingchong Liu, Zhonghai Yang, Hui Wang, and Z. F. Ren; Field Emission from Few-Layer Graphene Nanosheets Produced by Liquid Phase Exfoliation of Graphite; Journal of Nanoscience and Nanotechnology, 2010, Vol. 10, pp. 5051-5055.

[36] S. Goswami, U.N. Maiti, S. Maiti, S. Nandy, M.K. Mitra, K.K. Chattopadhyay ; Preparation of graphene–polyaniline composites by simple chemical procedure and its improved field emission properties; Carbon, 2011, Vol. 49, pp. 2245-52.

[37] Chandra Sekhar Rout, Padmashree D. Joshi, Ranjit V. Kashid, Dilip S. Joag, Mahendra A. More, Adam J. Simbeck, Morris Washington, Saroj K. Nayak, Dattatray J. Late; Superior Field Emission Properties of Layered WS2-RGO Nanocomposites; Scientific Reports, 2013, Vol. 3, pp. 3282.

[38] NM Huang, HN Lim, CH Chia, MA YarmoMR Muhamad; Simple room-temperature preparation of high-yield large-area graphene oxide; International Journal of Nanomedicine, 2011, Vol. 6, pp. 3443-3448.

[39] Laxmidhar Besra, Meilin Liu: A review on fundamentals and applications of electrophoretic deposition (EPD), Progress in Materials Science, 2007, Vol. 52, pp. 1–61.

[40] Robert Gomer : Field emission and field ionization, 1961, Harvard university press, Cambridge, Massachusetts, pp.10-45.

[41] Daniela C. Marcano, Dmitry V. Kosynkin, Jacob M. Berlin, Alexander Sinitskii, Zhengzong Sun, Alexander Slesarev, Lawrence B. Alemany, Wei Lu, and James M. Tour; Improved Synthesis of Graphene Oxide; ACS NANO, 2010, Vol. 4, No. 8, pp. 4806-4814.

[42] R. H. Fowler, F.R.S., and Dr. L. Nordheim: Electron Emission in Intense Electric Fields, Proc. Roy. Soc., 1928, series A, Vol. 119, no. 781, pp. 173.

[43] Zengcai Song,ab Hongwei Lei,a Borui Li,a Haoning Wang,a Jian Wen,a Songzhan Lia and Guojia Fang: Enhanced field emission from in situ synthesized 2D copper sulfide nanoflakes at low temperature by using a novel controllable solvothermal preferred edge growth route, Phys. Chem. Chem. Phys., 2015, Vol. 17, pp. 11790-11795.

[44] Dongxing Yanga, Aruna Velamakannia, Gu lay Bozoklub, Sungjin Parka, Meryl Stollera, Richard D. Pinera, Sasha Stankovichc, Inhwa Junga, Daniel A. Fieldd, Carl A. Ventrice Jr.d, Rodney S. Ruoffa; Chemical analysis of graphene oxide films after heat and chemical treatments by X-ray photoelectron and Micro-Raman spectroscopy; Carbon, 2009, Vol. 47, pp. 145-152.

[45] Goki Eda and Manish Chhowalla; Chemically Derived Graphene Oxide: Towards Large-Area Thin-Film Electronics and Optoelectronics; Adv. Mater., 2010, Vol. 22, pp. 2392-2415.

[46] Wufeng Chen and Lifeng Yan; Preparation of graphene by a low-temperature thermal reduction at atmosphere pressure; Nanoscale, 2010, Vol. 2, pp. 559-563.

[47] Mei Wang, Le Dai Duong, Joon-Suk Oh, Nguyen Thi Mai, Sanghoon Kim, Seungchul Hong, Taeseon Hwang, Youngkwan Lee and Jae-Do Nam; Large-Area, Conductive and Flexible Reduced Graphene Oxide (RGO) Membrane Fabricated by Electrophoretic Deposition (EPD); ACS Appl. Mater. Interfaces, 2014, Vol. 6, pp. 1747-1753.

[48] Eun-Young Choi, Tae Hee Han, Jihyun Hong, Ji Eun Kim, Sun Hwa Lee, Hyun Wook Kim and Sang Ouk Kim ; Noncolvalent Functionalization of Graphene with End-Functional Polymers; J. Mater. Chem., 2010, Vol. 20, pp. 1907-1912.

[49] Minoo Naebe, Jing Wang, Abbas Amini, Hamid Khayyam, Nishar Hameed, Lu Hua Li, Ying Chen & Bronwyn Fox; Mechanical Property and Structure of Covalent Functionalised Graphene/Epoxy Nanocomposites; Scientific Reports, 2014, Vol. 4, pp. 4375.

[50] Peng Cui, Junghyun Lee, Eunhee Hwang and Hyoyoung Lee; One-pot reduction of graphene oxide at subzero temperaturesw; Chem. Commun., 2011, Vol. 47, pp. 12370-12372.

[51] Mei Wang, Le Dai Duong, Nguyen Thi Mai, Sanghoon Kim, Youngjun Kim, Heewon Seo, Ye Chan Kim, Woojin Jang, Youngkwan Lee, Jonghwan Suhr and Jae-Do Nam; All-Solid-State Reduced Graphene Oxide Supercapacitor with Large Volumetric Capacitance and Ultralong Stability Prepared by Electrophoretic Deposition Method; ACS Appl. Mater. Interfaces, 2015, Vol. 7, pp. 1348-1354.